

Increasing electron density through n-type semiconductor to accelerate hot electrons from plasmonic Au nanospheres for artificial photosynthesis and cross-coupling reactions

Dinesh Kumar,^{a,b,c,d} Richa Jaswal,^{a,d,e} Devendra Shrestha,^c Suresh Kumar,^f Chan Hee Park,^{a,b,c,*} and Cheol Sang Kim^{a,c,*}*

^aDivision of Mechanical Design Engineering, Jeonbuk National University, Jeonju 54896, South Korea.

^bRegional Leading Research Center for Nanocarbon-based Energy Materials and Application Technology, Jeonbuk National University, Republic of Korea

^cDepartment of Bionanotechnology and Bioconvergence Engineering, Graduate School, Jeonbuk National University, Jeonju 54896, South Korea.

^dDepartment of Bionanosystem Engineering, Graduate School, Jeonbuk National University, Jeonju 54896, South Korea.

^eSchool of Pharmacy, Jeonbuk National University, Jeonju 54896, South Korea.

^fDepartment of Physics, NSCBM Government College Hamirpur, Himachal Pradesh 177005, India.

*Corresponding authors: E-mail: dineshkumar@jbnu.ac.kr (DK), biochan@jbnu.ac.kr (CHP)

This file contains 16 figures (Fig. S1-S16).

1. Materials and methods

Gold (III) chloride hydrate (99.99% trace metals basis), sodium stannate ($\text{Na}_2\text{SnO}_3 \cdot 3\text{H}_2\text{O}$, $\geq 99\%$), sodium citrate ($\geq 99.0\%$), and sodium hydroxide ($\geq 98.0\%$), were purchased from Sigma-Aldrich, USA. HR-TEM (JEOL-2010, Japan, 200 kV) was used for HRTEM analysis. Extinction spectra were obtained with a UV spectrometer (SCINCO, South Korea). Structural analyses were performed using X-ray diffraction (Rigaku D/MAX 2500Tokyo, Japan). The amount of CO_2 dissolved in the reaction samples was determined using an HI 3818 carbon dioxide test kit (Hanna Instruments, Romania). ^1H -NMR and ^{13}C -NMR analyses were carried out using a JEOL JNM AL-400 instrument. The GC-MS analysis was carried out on Agilent 7890A GC and Agilent 5975C mass selective detector (Agilent Technologies, Santa Clara, CA, USA). Fourier transform infrared (FT-IR) spectra were recorded on a Jasco FTIR-4200 spectrophotometer (Maryland, USA). Renishaw, Raman microsystem 2000 (Derbyshire, England) was used for the Raman analysis. High-performance liquid chromatography (HPLC) with a UV detector and an automatic injector has been utilized for the analysis of the coupling reaction products. ZORBAX column (150 mm \times 3.0 mm, 3.5 μm) was used with a 70% aqueous acetonitrile eluent. The flow rate was 1.0 mL per minute.

2. Photo-catalytic reactors

A Xe lamp (Ceramaxs, Waltham, USA) with a power density of 6.0 W/cm^2 was used as a visible light (370-770 nm) source. In addition, a near-infrared (NIR) laser (OCLA Laser, Passive Cooled InGaAs diode laser, LaserLab[®] South Korea, 808 nm, output power = 3.0 W/cm^2) was used. A solar simulator (Newport) with a power density of 1.2 W/cm^2 was used.

3. CO₂ reduction under H₂ gas flow

CO₂ reduction was carried out in the presence of a continuous flow of H₂ for 3 h without light irradiation. H₂ gas was generated by adding an aluminum foil to NaOH solution (200 mL, 2.0 M).⁴ The as-generated H₂ gas was passed into CO₂-saturated distilled water continuously for 3 h. Then, after adjusting the pH to 12.0 with dilute NaOH, the solution evaporated to dryness. The product was analyzed by ¹H-NMR and ¹³C-NMR.

4. CO₂ photo-conversion reaction product analysis

After the completion of the reaction (5 h), the resulting reaction mixture was centrifuged at 9,000 rpm/15 min to remove nanoparticles and to obtain the supernatant-containing product. Then the solution was analysed with gas chromatography-mass spectrometry (GC-MS). For GC analysis, the oven temperature was varied from 35 °C to 100 °C using helium gas as the carrier gas with an injector temperature of 200 °C and a sampling time of 20 min for GC-MS analysis. The equation obtained from the standard deviation curve was used to calculate the number of moles of formic acid formed.

Also, the pH of the resulting reaction mixture was adjusted to 12 by the addition of a dilute NaOH solution to convert HCOOH to sodium formate (HCOO⁻Na⁺). After rotary evaporation, the final product was analysed with ¹H-NMR, ¹³C-NMR (600 MHz, CDCl₃), FTIR, and Raman spectroscopic studies. The quantum yield (QY) and chemical yield (CY) were calculated using GC and ¹H-NMR analysis techniques.

The small aliquots (10 µL) of CO₂ reduction reaction mixtures were placed on a quartz substrate and allowed to dry and then analyzed for Raman spectroscopy (the samples were analyzed with 532 nm laser excitation (50 mW)). Spectral data were collected over the range 400–1800 cm⁻¹

with 10 sec of integration time.

5. Chemical and quantum yield calculation

5.1. Chemical yield calculation

(1) The amount of CO₂ in the 10 mL solution was found to be 2.4 mg, as calculated by using a carbon dioxide kit (HI 3818, Hanna Instruments, Romania) and the procedure given along with it. The titration flask was rinsed with a CO₂-purged aqueous sample (5 mL) and 1 drop of phenolphthalein indicator was added. There was no change in the color of the indicator solution observed. After that, the mixture was titrated with the HI 3818-0 solution provided by the carbon dioxide kit until the emergence of a pink color. The total amount consumed for the titration was multiplied by 100 to obtain the quantity (ppm) of CO₂. The experiment was repeated three times.

(2) The quantification of formic acid was carried out using a standard deviation curve plotted using ¹H-NMR (five standard samples of formic acid in CDCl₃ with increasing concentrations ranging from 0.015 mM to 0.15 mM) and GC-MS analysis.

(3) The chemical yield was calculated by dividing the molar concentration of formic acid formed by the molar concentration of carbon dioxide dissolved in the reaction sample. For example:

The equation obtained from the standard deviation curve (NMR): -

Moles of HCOOH ÷ 10 mL = 0.00011 M (from standard deviation curve)

Moles of CO₂ ÷ 10 mL = 0.005455 M (calculated using the carbon dioxide kit)

Chemical yield = moles of HCOOH ÷ Moles of CO₂ × 100

= 0.00011 ÷ 0.005455 × 100 = 2.016% (i)

5.2. The quantum yield (QY) of produced formic acid was calculated by using the following equation:

$$\text{QY (\%)} = \text{number of reacted electrons} \div \text{number of incident photons} \times 100\%$$

$$= 2 \times \text{number of formic acid molecules} / \text{number of incident photons} \times 100\% \quad (\text{ii})$$

$$\text{Number of incident photons} = \text{moles of Fe}^{2+} \div \phi_{\lambda} \times t \times F \quad (\text{iii})$$

(Moles of Fe^{2+} (calculated) = 0.03588, ϕ_{λ} = quantum yield of Fe^{2+} ion concentration = 0.65, t = time = 20 s,

F = mean fraction of light absorbed by ferrioxalate solution = 0.1488

$$\text{Number of incident photons} = 0.03588 \div 0.65 \times 20 \times 0.1488$$

$$= 0.01855 \text{ photons s}^{-1} \quad (\text{iv})$$

$$\text{QY (\%)} = 2 \times \text{number of formic acid molecules} / \text{number of incident photons} \times 100\%$$

$$= 2 \times 0.00011 / 0.01855 \times 100 = 1.1859\% \quad (\text{v})$$

The number of incident photons was measured by the ferrioxalate actinometer method (equations (iii) and (iv)).¹⁻³ The actinometer solution was prepared as follows. In a 100-mL flask, an aqueous solution of $\text{Fe}_2(\text{SO}_4)_3$ (5 mL, 0.2 M) and an aqueous solution of $\text{K}_2\text{C}_2\text{O}_4$ (5 mL 1.2 M) were added. Then, this mixture was diluted to 100 mL volume by using distilled water. Then, the above actinometer solution (40 mL) was irradiated under visible light for 20 sec.

Consequently, the ferrous ion concentration was determined by the formation of the iron-phenanthroline complex, detected by UV-visible spectrophotometry at 510 nm. The analytical procedure was as follows. In a 100-mL flask, the actinometer solution (1 mL) after irradiation, an aqueous solution of 1,10-phenanthroline (2 mL, 0.2 wt %), and a buffer solution (0.5 mL) of pH =

4–5 was mixed and diluted to 100 mL with distilled water and kept in the dark for 30 min. After 30 min, the absorbance of the solution at 510 nm was measured using a UV-visible spectrophotometer. A comparative test was conducted by following the above-mentioned procedure for the blank solution (actinometer solution without irradiation), and the ferrous ion concentration was calculated by UV-visible spectrophotometric observation at 510 nm.

5.3. Determination of apparent quantum efficiency (AQE)

Under different monochromatic light wavelengths (450, 550, and 650 nm) irradiation, the values of light intensities are measured to 3.36, 3.28, and 3.65 mW/cm² corresponding to the 450, 550, and 650 nm incident wavelength, respectively. The HCOOH yields are measured after 5.0 h of photocatalytic reaction, and the AQE is calculated on the basis of the following equation⁴:

$$\text{AQE} = \text{Number of reacted electrons} / \text{Number of incident photons} = \text{Number of generated HCOOH} \times 2 / \text{Number of incident photons} = M \cdot N_A \cdot 2 / (I \times A \times t / h\nu)$$

Where M represents the amount of HCOOH generation, N_A represents Avogadro's constant, I is the light intensity, A is the light incident area (1 cm²), t is light irradiation time, h and ν are Planck constant and the incident light frequency, respectively.

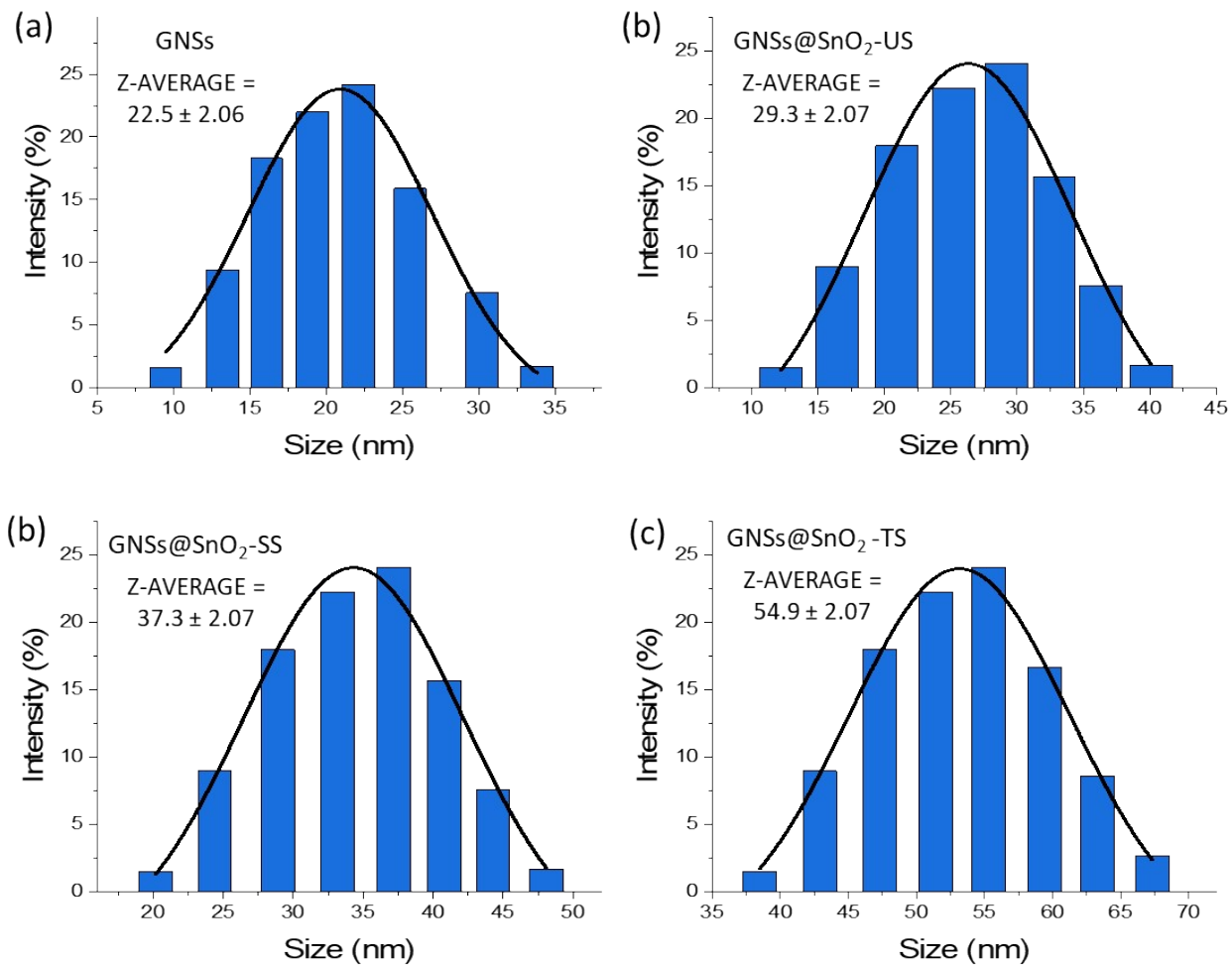


Fig. S1. Dynamic light scattering (DLS) analysis of (a) GNSs, (b) GNSs@SnO₂-US, (c) GNSs@SnO₂-SS, and (d) GNSs@SnO₂-TS nanoparticles.

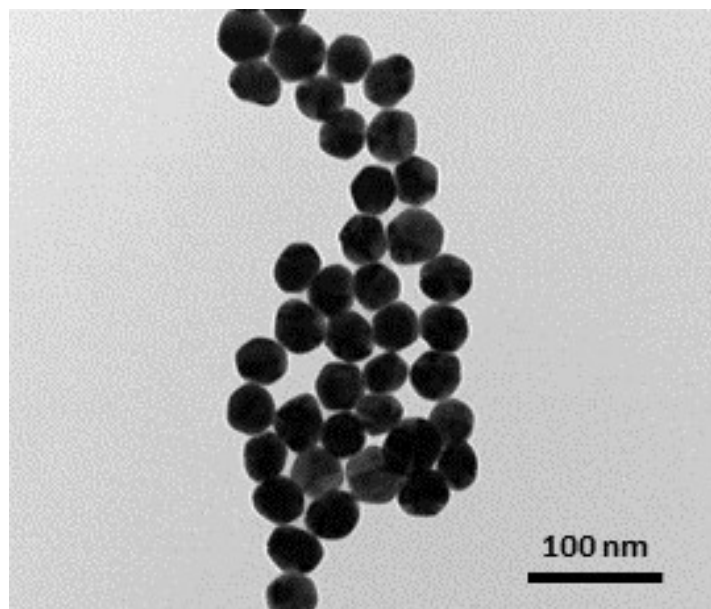


Fig. S2. TEM image of prepared gold nanospheres (GNSs).

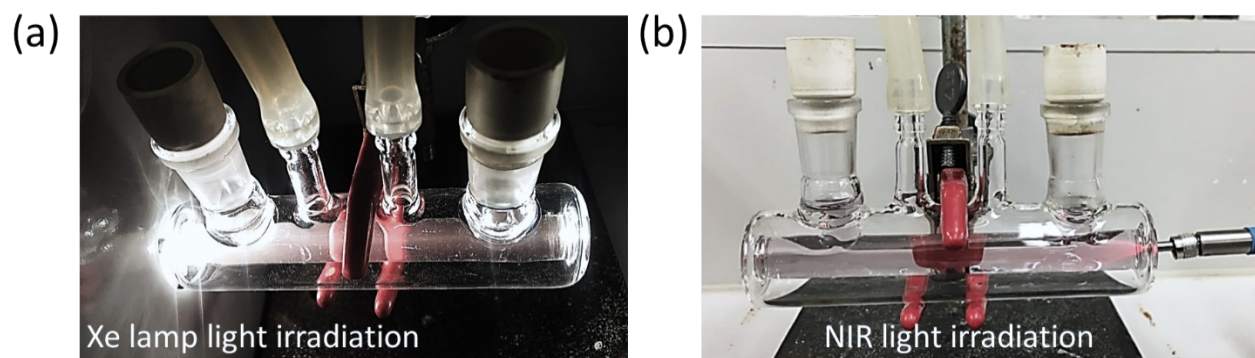


Fig. S3. The Pyrex glass reactor with water circulation jacket under **(a)** Xe lamp (visible light) and **(b)** NIR light.

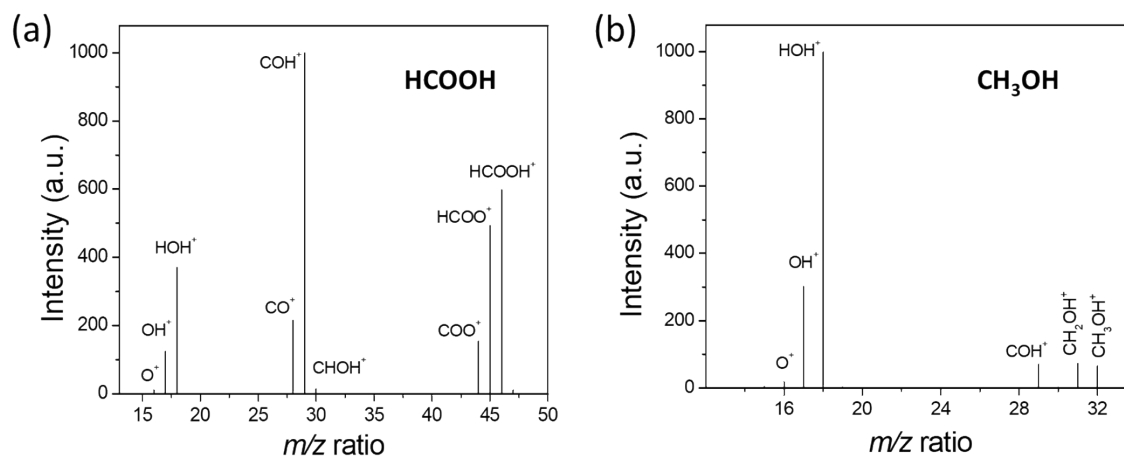


Fig. S4. Mass spectrum of **(a)** formic acid (HCOOH) and **(b)** methanol (CH₃OH) generated from the GNSs@SnO₂-SS mediated CO₂ photoconversion.

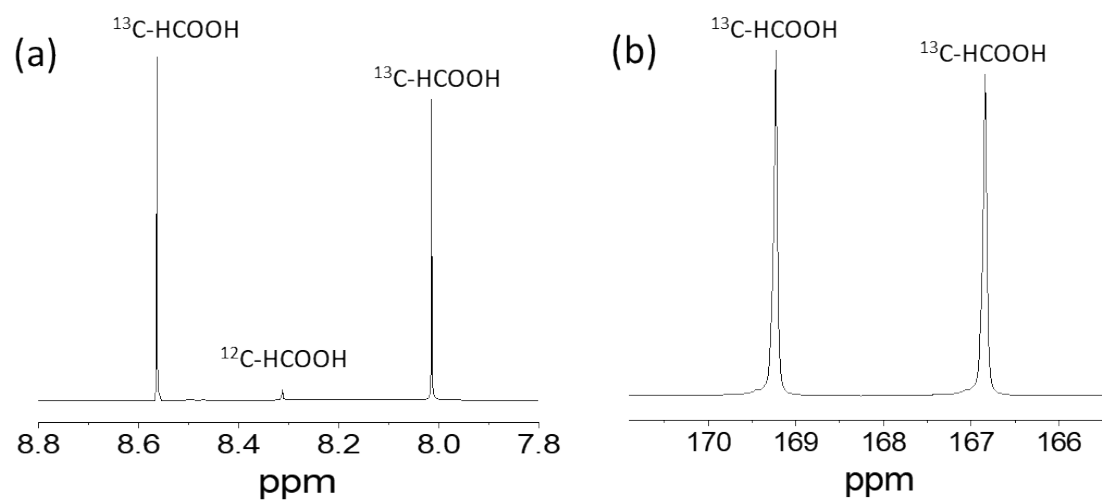


Fig. S5. (a) ^1H -NMR spectra and (b) ^{13}C -NMR spectra for the HCOOH generated from the photocatalytic conversion of isotopic $^{13}\text{CO}_2$ gas.

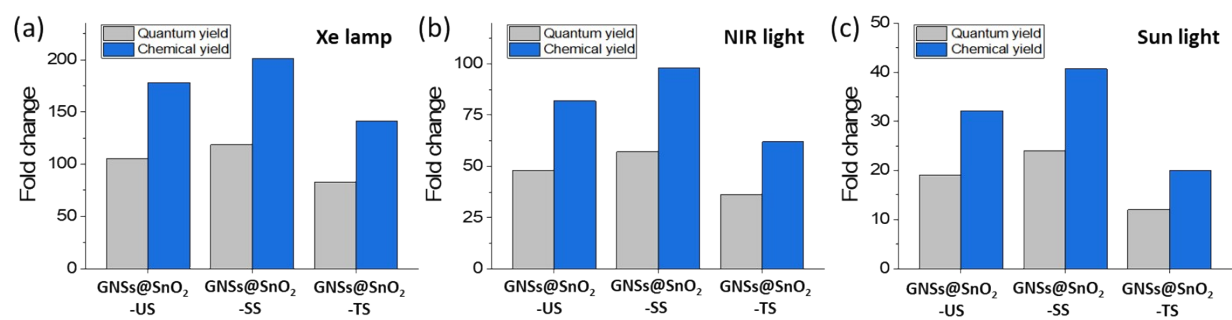


Fig. S6. CO₂ conversion fold change under **(a)** visible, **(b)** NIR, and **(c)** solar light irradiation using GNSs@SnO₂-US, GNSs@SnO₂-SS, and GNSs@SnO₂-TS nanoparticles.

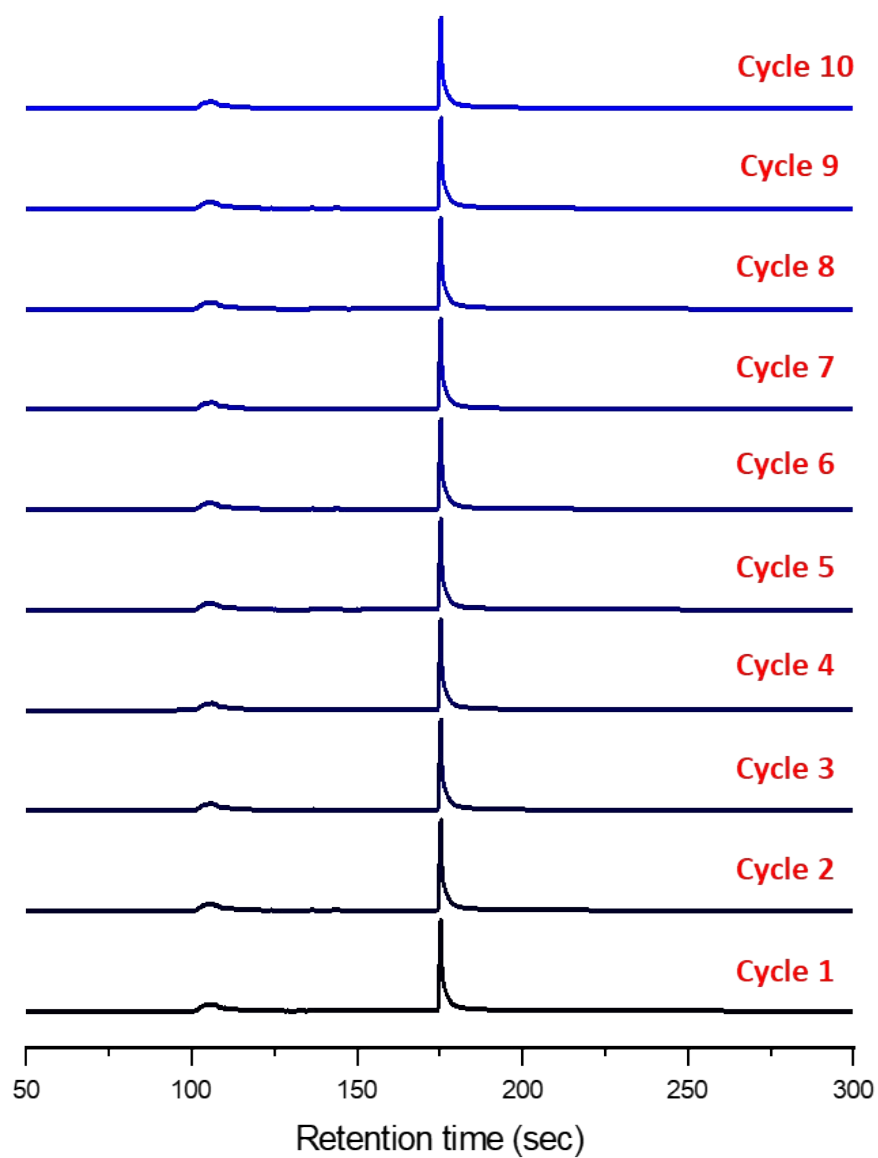


Fig. S7. Gas chromatogram of ten reaction cycles of GNSs@SnO₂-SS mediated CO₂ photoconversion.

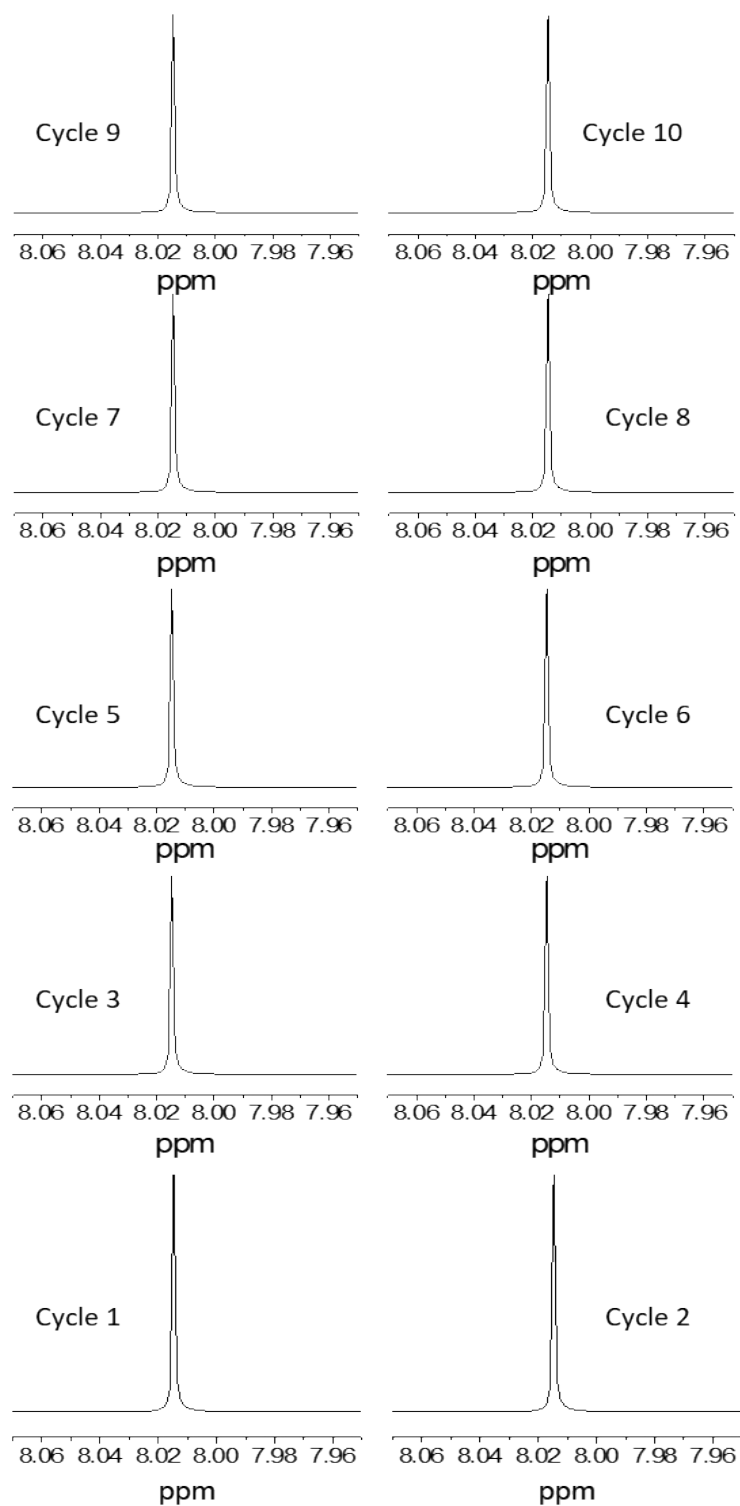


Fig. S8. ^1H -NMR spectra of ten reaction cycles of GNSs@SnO₂-SS mediated CO₂ photoconversion.

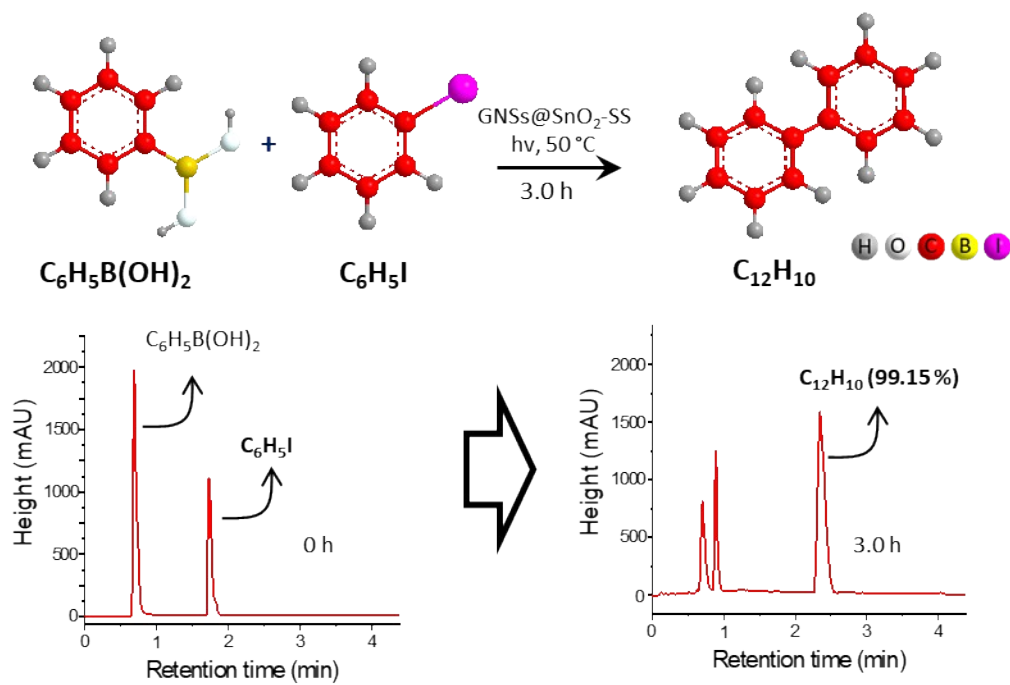


Fig. S9. The Suzuki-Miyaura coupling reaction in the presence of $GNSs@SnO_2-SS$ with schematic and HPLC chromatogram.

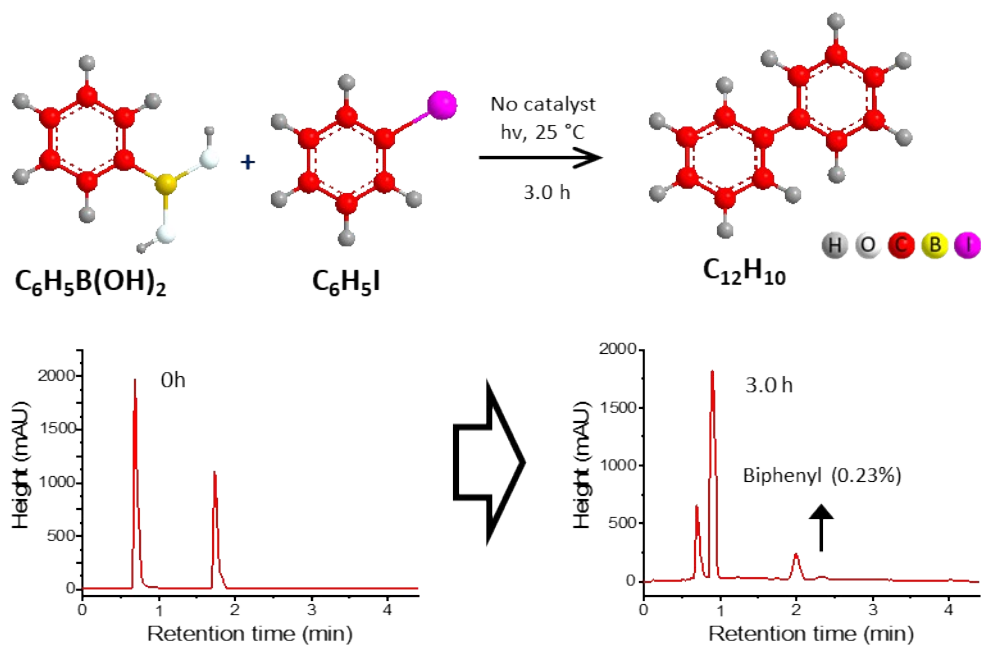


Fig. S10. The Suzuki-Miyaura coupling reaction at room temperature without any photocatalyst with schematic and HPLC chromatogram.

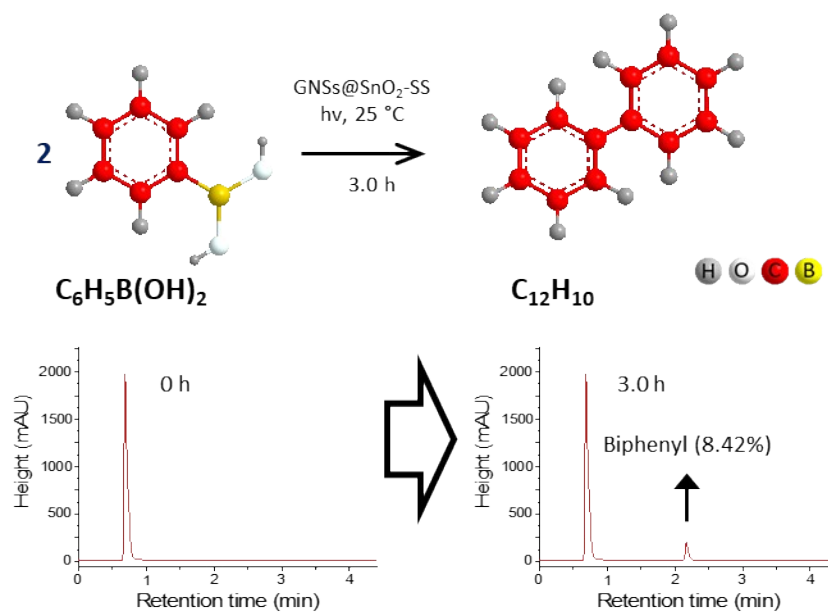


Fig. S11. The coupling reaction of only phenylboronic acid at room temperature with schematic and HPLC chromatogram.

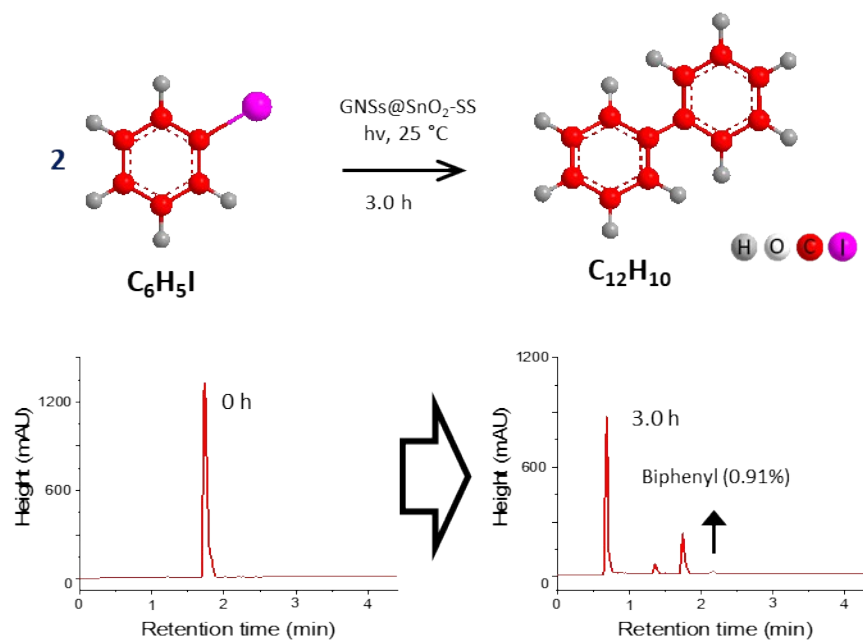


Fig. S12. The coupling reaction of only iodobenzene at room temperature with schematic and HPLC chromatogram.

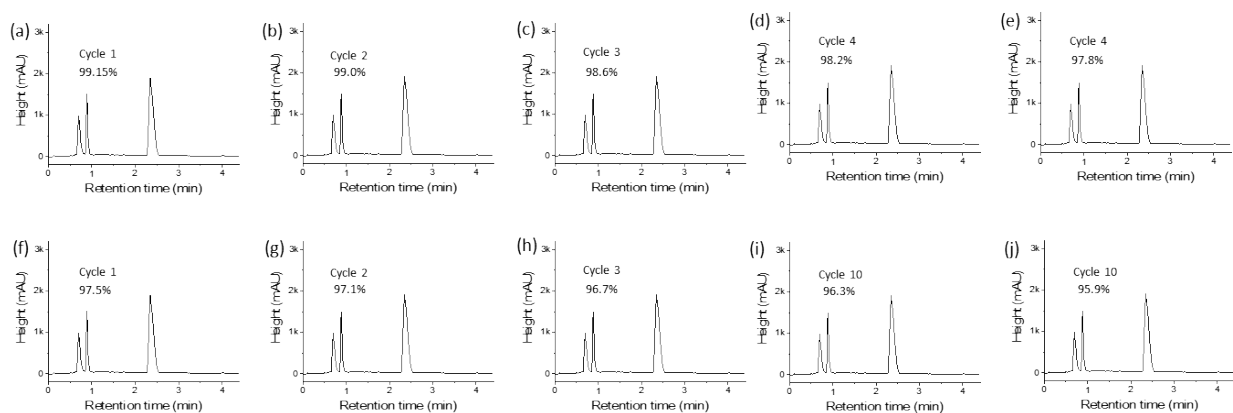


Fig. S13. HPLC chromatograms of (a) first, (b) second, (c) third, (d) fourth, (e) fifth, (f) sixth, (g) seventh, (h) eighth, (i) ninth, and (j) tenth GNSs@SnO₂-SS mediated visible light-induced Suzuki-Miyaura coupling reaction cycle.

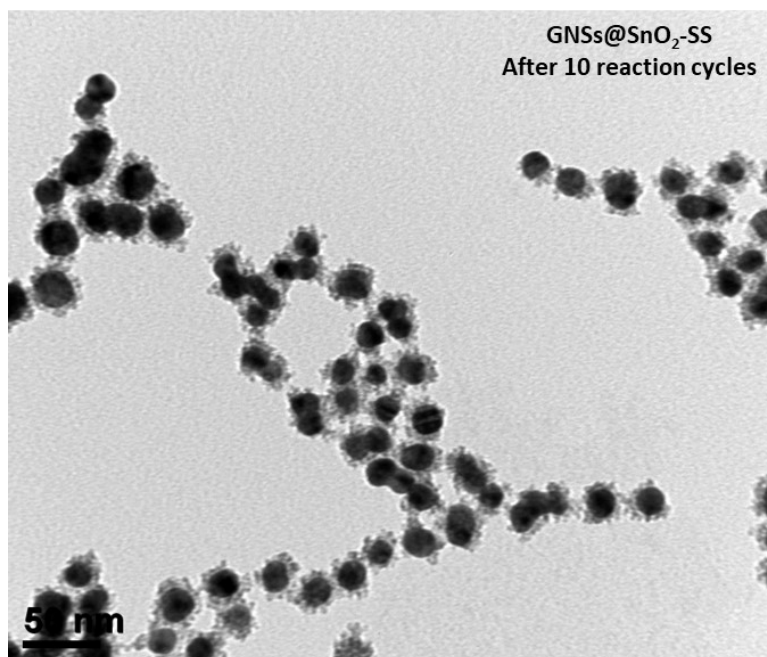


Fig. S14. TEM image of GNSs@SnO₂-SS after 10 reaction cycles.

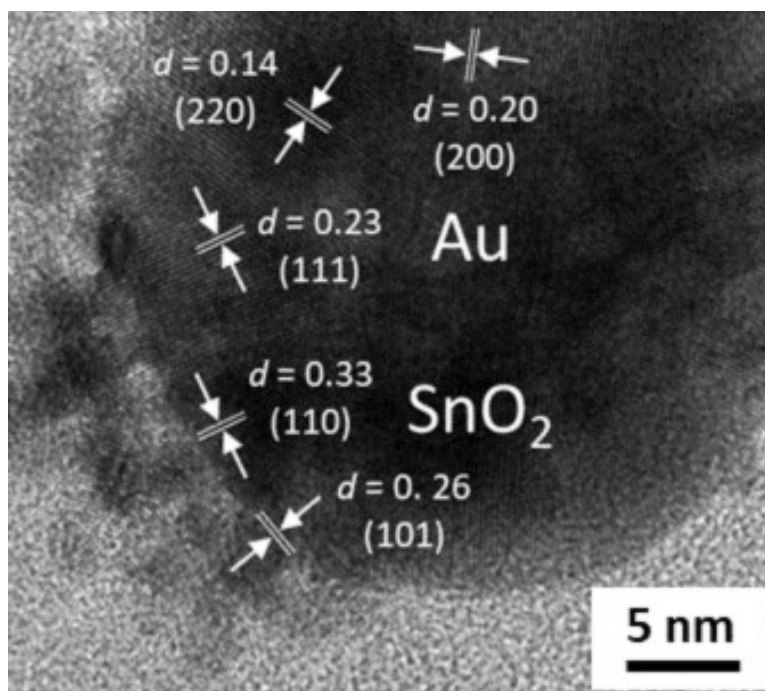


Fig. S15. HRTEM image of recycled GNSs@SnO₂-SS.

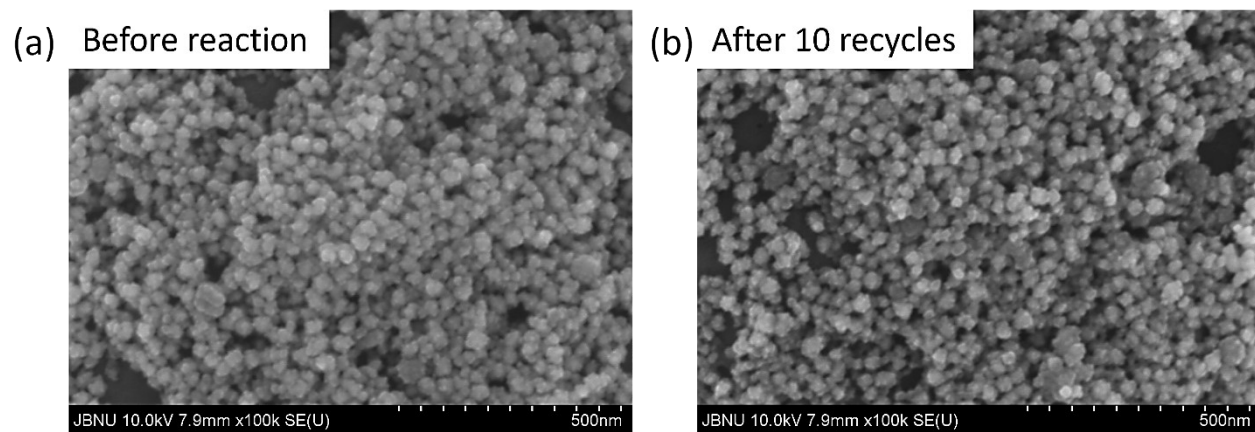


Fig. S16. FESEM images of (a) fresh and (b) recycled GNSs@SnO₂-SS nanoparticles.

References

1. C. An, J. Wang, W. Jiang, M. Zhang, X. Ming, S. Wang and Q. Zhang, *Nanoscale*, 2012, **4**, 5646-5650.
2. D. Kumar, A. Lee, T. Lee, M. Lim and D.-K. Lim, *Nano Letters*, 2016, **16**, 1760-1767.
3. M. Schiavello, V. Augugliaro, V. Loddo, M. J. López-Muñoz and L. Palmisano, *Research on Chemical Intermediates*, 1999, **25**, 213-227.
4. H. Yin and J. Li, *Applied Catalysis B: Environmental*, 2023, **320**, 121927.